# Sorption of Butane on Carbon Multiwall Nanotubes at Room Temperature

Jenny Hilding, Eric A. Grulke,* Susan B. Sinnott,† Dali Qian, Rodney Andrews, and Marit Jagtoyen

*Chemical and Materials Engineering, Center for Applied Energy Research, University of Kentucky, Lexington, Kentucky 40506*

*Received January 25, 2001. In Final Form: July 26, 2001*

Carbon multiwall nanotubes (MWNTs) can be used for separation processes if the mechanisms for sorption and desorption are known. This study describes the sorption mechanism for butane on MWNTs at room temperature and relative pressures ranging from 0 to 0.9. Previous workers have studied the sorption of hydrogen,[1−3] neon,[4−6] helium,[6] nitrogen,[7] and methane[8−10] on nanotubes for storage purposes. Molecular dynamic simulations have been done to show that carbon nanotubes can be used as a separation tool to selectively separate isomers of monomethylnaphthalenes.[11] Experiments have established that refrigerant mixtures, such as $CHF_2CF_3$ and $CClF_2CF_3$, can be successfully separated by using carbon nanotubes.[12] Previous work in this lab has shown that carbon MWNTs can separate butane from methane when both are at low levels in a gas flow. This experimental result is in agreement with recent molecular dynamic simulations made for sorption of alkane mixtures on different types of single-walled carbon nanotubes (SWNTs).[13] Morphology characterization of the MWNTs has been used to interpret the sorption data. Most of the butane was sorbed to the external surface of the MWNTs and only a small fraction of the butane condensed in the pores. No hysteresis was observed between sorption and desorption experiments. The weight fraction of butane sorbed depended inversely on the diameter of the MWNTs and was 5.3 wt % for one of the samples studied. Adsorption isotherms were modeled using a modified BET equation with coefficients consistent with the known morphology. Fixed bed adsorption systems that could use the exterior surface of MWNTs might be attractive for separations, particularly if electrical heating could be used for rapid desorption of sorbed molecules.

## Introduction

Carbon nanotubes have generated increasing interest during the recent decade due to their unique properties, such as uniform porosity, high tensile strength, electrical conductivity, and relative inertness. Single-wall nanotubes and MWNTs have regular and controllable geometries that could be used to develop precise separation tools. If the sorption mechanisms are known, then we should be able to control sorption of various gases through combinations of temperature, pressure, and nanotube morphology. Since the large-scale production of carbon nanotubes is now constantly progressing[14−20] and may result in moderate costs, precise separation methods based on carbon nanotubes should be investigated. The mechanism of adsorption in capillary cores and surface adsorption must first be evaluated in order to investigate these possibilities.

Sorption of hydrogen on SWNTs, MWNTs, and surface-treated MWNTs has been proposed as a storage mechanism. SWNTs are thought to store hydrogen by sorption between nanotubes within bundles and/or inside the nanotube pores. Many SWNT samples contain varying amounts of bundle sizes and bundle lengths (which can be varied by grinding and other mechanical operations) as well as contaminating amorphous carbon. Therefore, gas sorption on any particular sample is very dependent on its prior history and the sample morphology. On the other hand, MWNTs can be made in uniform lengths, with known diameter distributions, without bundle formation, and with essentially no amorphous carbon. We have chosen to study the uptake of an alkane on high-purity, well-characterized MWNTs to determine the sorption mechanisms and to develop sorption models for these new materials.

Carbon MWNTs are produced at the Center for Applied Energy Research using chemical vapor deposition (CVD).[14,15] This technique produces aligned nanotube mats with no bundle formation, very few nanotube contact

* Corresponding author. E-mail: egrulke@engr.uky.edu. Phone: (859) 257-4958.

† Present address: University of Florida, Department of Materials Science and Engineering, Gainesville, FL 32611-6400.

(1) Liu, C.; Fan, Y. Y.; Liu, M.; Cong, H. T.; Cheng, H. M.; Dresselhaus, M. S. *Science* **1999**, *286*, 1127.

(2) Chen, P.; Wu, X.; Lin, J.; Tan, K. L. *Science* **1999**, *285*, 91.

(3) Dillon, A. C.; Jones, K. M.; Bekkedahl, T. A.; Kiang, C. H.; Bethune, D. S.; Heben, M. J. *Nature* **1997**, *386*, 377.

(4) Teizer, W.; Hallock, R. B.; Dujardin, E.; Ebbesen, T. W. *Phys. Rev. Lett.* **2000**, *84*, 1844.

(5) Teizer, W.; Hallock, R. B.; Dujardin, E.; Ebbesen, T. W. *Phys. Rev. Lett.* **1999**, *82*, 5305.

(6) Stan, G.; Crespi, V. H.; Cole, M. W.; Boninsegni, M. *J. Temp. Phys.* **1998**, *113*, 447.

(7) Inoue, S.; Ichikuni, N.; Suzuki, T.; Uematsu, T.; Kaneko, K. *J. Phys. Chem. B* **1998**, *102*, 4689.

(8) Weber, S. E.; Talapatra, S.; Journat, C.; Zambano, A.; Migone, A. D. *Phys. Rev. B* **2000**, *61*, 13150.

(9) Muris, M.; Defau, N.; Bienfait, M.; Dupont-Pavlovsky, N.; Grillet, Y.; Palmari, J. P. *Langmuir* **2000**, *16*, 7019.

(10) Benfait, M.; Asmussen, B.; Johnson, M.; Zeppenfeld, P. *Surf. Sci.* **2000**, *460*, 243.

(11) Takaba, H.; Katagiri, M.; Kubo, M.; Vetrivel, R.; Miyamoto, A. *Microporous Mater.* **1995**, *3*, 449.

(12) Corbin et al. US Pat. 5,648,569, 1997.

(13) Mao, Z.; Sinnott, B. Submitted to *J. Phys. Chem. B.*

(14) Andrews, R.; Jacques, D.; Rao, A. M.; Debyshire, F.; Qian, D.; Fan, X.; Dickey, E. C.; Chen, J. *Chem. Phys. Lett.* **1999**, *303*, 467.

(15) Jacques, D.; Villain, S.; Rao, A. M.; Andrews, R.; Debyshire, F.; Dickey, E. C.; Qian, D. *Mater. Res. Soc. Symp. Proc.* **2000**, *593*, 15.

(16) Rao, A. M.; Jacques, D.; Haddon, R. C.; Zhu, W.; Bower, C.; Jin, S, *Appl. Phys. Lett.* **2000**, *76*, 3813.

(17) Andrews, R.; Jacques, D.; Rao, A. M.; Rantell, T.; Derbyshire, F.; Chen, Y.; Chen, J.; Haddon, R. C. *Appl. Phys. Lett.* **1999**, *75*, 1329.

(18) Qian, D.; Dickey, E. C.; Andrews, R.; Rantell, T. *Appl. Phys. Lett.* **2000**, *76*, 2868.

(19) Sinnott, S. B.; Andrews, R.; Qian, D.; Rao, A. M.; Mao, Z.; Dickey, E. C.; Derbyshire, F. *Chem. Phys. Lett.* **2000**, *315*, 25.

(20) Rao, A. M.; Jacques, D.; Haddon, R. C.; Zhu, W.; Bower, C.; Jin, S. *Appl. Phys. Lett.* **2000**, *76*, 3813.

10.1021/la010131t CCC: $20.00 
Published on Web 11/03/2001

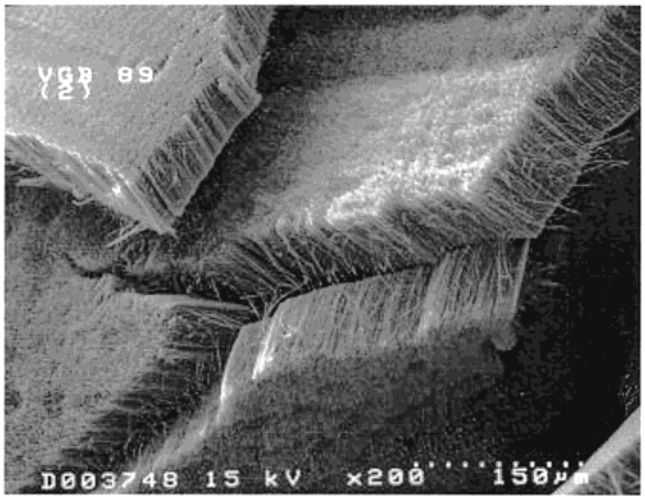


**Figure 1.** SEM picture showing MWNT length.


**Figure 2.** SEM picture showing the variety of outer diameter for MWNTs.

points, homogeneous lengths, and well-defined diameters (Figures 1−3). Figure 1 illustrates the uniform length of nanotubes made by the CVD process. Figure 2 shows the nanotube diameter distribution and demonstrates that, in contrast to SWNTs, these MWNTs do not associate in bundles. The MWNTs have a purity of >95%. (The nonnanotube component is the remnant of the iron catalyst used to grow the nanotubes.) The reactor product has uniform lengths (50−55 $\mu$m) and all dimensions (internal diameter, external diameter, and length) can be varied with reaction conditions. Figure 3 is a TEM picture of the MWNT pore. As can be seen, the pore is centered at the core of the MWNT, and the diameter of the pore is large compared to the distance between the multiple graphite layers. There is essentially no amorphous carbon within the mats or adhering to the nanotube exteriors.

Since the MWNTs are electrically conducting, controlled currents can be used to heat a nanotube adsorption bed, resulting in very rapid desorption and low cycle times in fixed bed operations, an advantage compared to activated carbons, which usually are nonconductive. However, the small size of the MWNTs is a potential disadvantage, since they would have to be immobilized in a practical flow process. This study determines the sorption mechanism for butane on MWNTs as a first step toward investigating a hydrocarbon separation process.

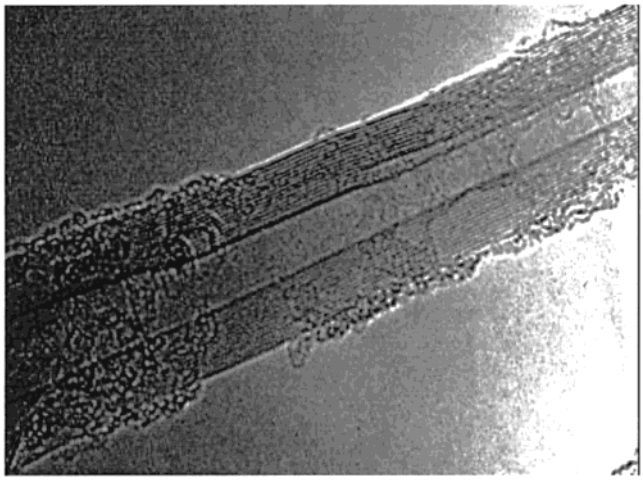

**Figure 3.** TEM picture showing the pore at the core of a MWNT.

## Experimental Section

**Multiwalled Nanotubes.** The MWNTs used were produced at CAER (Center for Applied Energy Research) through chemical vapor deposition.[14,15] Three samples with similar lengths but different diameter distributions were used. The MWNTs were cut from their substrate, so that all nanotubes were open to the atmosphere. The pore diameters and the external diameters were measured sample in TEM micrographs (JEOL, JEM-2000 FX electron microscope) for a hundred different nanotubes of each sample.

**Butane Adsorption.** Adsorption isotherms were determined in a Hiden instrument (IGA-002). The sample (~45 mg) was hung in a small quartz bulb connected to a microbalance. Sorbed water and other gases were removed by heating the system to 473.15 K at atmospheric pressure. At this temperature, the vapor pressure of water in the capillary pores exceeded the saturation conditions, as calculated from the Kelvin equation using vapor pressure, liquid density, and surface tension from the DIPPR data set.[21]

After degassing, the system was cooled to 298.15 K for sorption studies. The pressure of the system was decreased to 0.2 mbar (corresponding to a relative pressure of $8 \times 10^{-5}$ for butane), and the system was left until the sample weight was stabilized and measured. The butane pressure was increased in small increments of 0.05% of the pressure span, and the sample was allowed to reach equilibrium after each step. The minimum hold time after a pressure change was set at 5 min. When the mass or pressure fluctuations were less than 0.02% of the span, the sample was deemed to be at equilibrium and the next step was taken. This procedure continued until the system reached the maximum cycle pressure of 2250 mbar, which is less than the saturated vapor pressure, $P_0$, for butane at 298.15 K (2437 mbar). Desorption curves were obtained by reducing the pressure in step changes to low final pressure values. Similar criteria were used for determining the equilibrium points.

The microbalance/microbalance controller of the Hiden has a sensitivity with an intrinsic accuracy equivalent to ±0.006% of the selected weighing range (100 mg in this case). The pressure control system can typically maintain a pressure set point to within 0.02% of the operating range. The thermoregulator has an accuracy of at least ± 0.1 °C, and the intrinsic resolution of the temperature sensor is in the range 0.1−0.25 K.

## Results

Carbon MWNTs have well-defined morphology that can be measured and modeled accurately. Pore volume and surface area distributions can be used in combination with the Kelvin and BET equations to predict the magnitudes of pore condensation and surface condensation mechanisms.

(21) Daubert, T. E.; Danner, R. P.; Sibul, H. M.; Stebbins, C. C. *Design Institute for Phys. Prop. Data A.I.Ch.E.* Taylor & Francis, 1989.

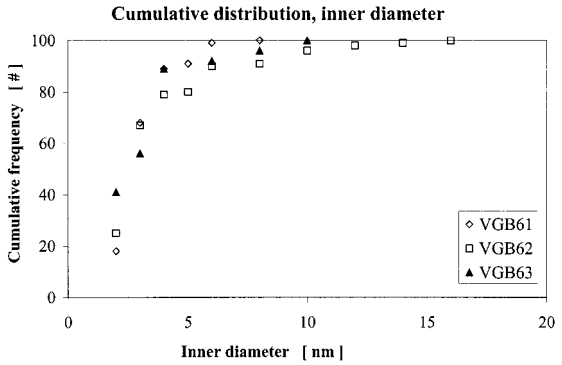


**Figure 4.** Cumulative distribution inner diameter, VGB61, VGB62, and VGB63 (D. Qian, UKY).

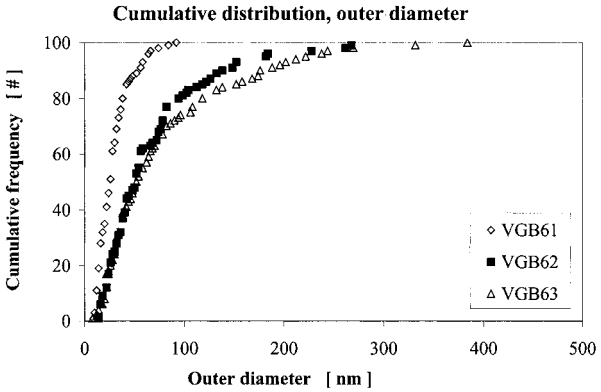


**Figure 5.** Cumulative distribution outer diameter, VGB61, VGB62, and VGB63 (D. Qian, UKY).

**MWNT Morphology.** The length of the MWNTs was uniform and in the range 50−55 $\mu$m. TEM photomicrographs established that the MWNTs are open at one end and that both inner and outer diameter differed quite a bit from tube to tube within a sample. Size distribution curves were developed by measuring internal and external diameters for a hundred MWNTs from each sample (Figures 4 and 5). Models were fitted to the cumulative distributions rather than the differential distributions because of the limited number of data points. Several different distributions were considered, but log-normal models clearly fit the data best (Table 1, Figure 6). The log-normal distribution accounts for the long "tail" of larger sized nanotubes. Previous workers have shown that MWNT diameters are directly related to the size of the iron catalyst nanoparticle.[14,15]

Table 1 lists the samples in the order of their mean outer diameters. VGB61 had a significantly smaller outer diameter than the other two, with a narrower distribution. The mean inner diameters were similar, but VGB61 had a narrower distribution of this dimension as well. By definition, the MWNT cores were strictly within the mesoporous range (radius 1−25 nm). From the estimated distributions for each sample, the pore volume, the internal surface area, and external surface area were calculated as presented in Table 1. For a sample with smaller outside diameters, pore volume and surface area per gram were expected to be larger than for MWNTs with larger outside diameters. For all samples, the pore volume was a small fraction of the solid volume, while the surface area differed significantly between the samples. By comparison, commercial activated carbons (AC) have typical surface areas in the range 1000 $m^2/g$ in microporous AC, 10−100 $m^2/g$ in mesoporous AC, and 1 $m^2/g$ in macroporous AC.

**Table 1. Geometrical and Quantitative Adsorption Calculations for VGB61, VGB62, and VGB63[a]**

| sample | VGB61 | VGB62 | VGB63 |
|---|---|---|---|
| sample weight [mg] | 44.71 | 49.23 | 44.42 |
| mean diameter [nm] | | | |
| internal | 2.64 | 2.65 | 2.40 |
| extenal | 24.33 | 48.67 | 53.18 |
| standard average error | | | |
| internal | 0.33 | 0.60 | 0.60 |
| external | 0.57 | 0.77 | 0.90 |
| pore vol [$m^3/g$] | 1.33E−09[b] | 1.48E−10 | 1.16E−10 |
| external surface area [$m^2/g$] | 37.9 | 14.8 | 11.2 |
| internal surface area [$m^2/g$] | 0.97 | 0.31 | 0.067 |
| total uptake [g butane/g MWNT] | 5.28E−02 | 2.08E−02 | 1.22E−02 |
| pore sorption [g butane/g MWNT] | 7.64E−07 | 8.51E−08 | 6.64E−08 |
| surface uptake [g butane/$m^2$ MWNT] | 1.39E−03 | 1.40E−03 | 1.14E−03 |

[a] The mean diameter and the standard average error are model parameters for a log-normal fit to cumulative diameter distributions for each sample. Pore volume and surface area for the samples are calculated from the log-normal fit. The butane uptake is measured at $P/P_0 = 0.90$. Pore and surface uptake calculations are based on the log-normal fit of the MWNT morphology together with physical data of butane. [b] Read as $1.33 \times 10^{-9}$.

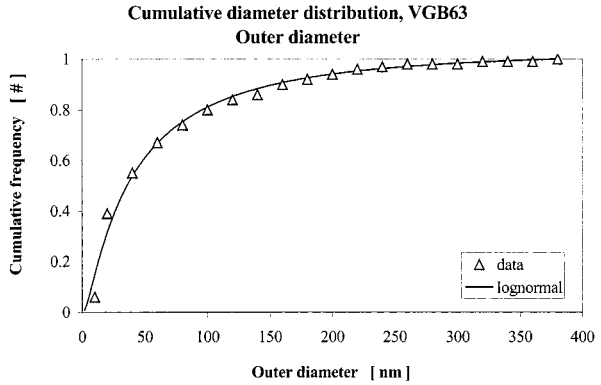


**Figure 6.** Graph showing a log-normal fit to cumulative diameter distribution for VGB63, external diameter.

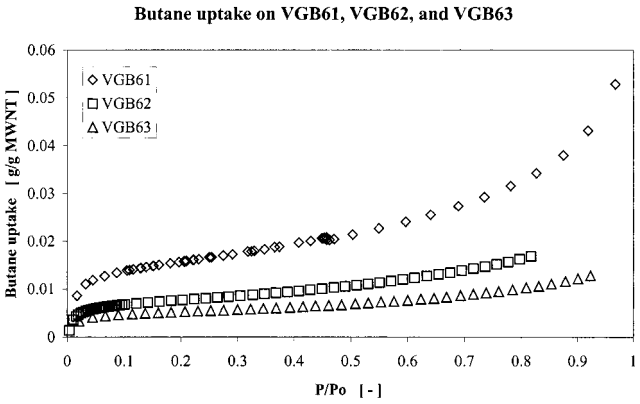


**Figure 7.** Butane sorption isotherms for three MWNT samples.

**Adsorption Isotherms.** Figure 7 shows the raw data of the sorption isotherms of butane on the three MWNT samples at 298.15 K and relative pressures from 0 to 0.90. The sorption isotherms were similar to isotherms previously reported for $N_2$ and $CH_4$ on carbon nanotubes.[7,22]

There are two sorption mechanisms for these samples: diffusion of butane into the pores accompanied by con-

(22) Mackie, E. B.; Wolfson, R. A.; Arnold, L. M.; Lafdi, K.; Migone, A. D. *Langmuir* **1997**, *13*, 7197.

densation and sorption of butane on the external surface of the MWNTs. Each mechanism may have a different characteristic time. The time needed for butane to diffuse into the nanotube pores can be estimated assuming unsteady-state diffusion through the pore based on a constant butane partial pressure at the pore mouth. For a pore length of 50 $\mu$m, a diffusivity of 0.1 cm$^2$/s, and a Fourier number for diffusion of ~1 (about 90% of the final step change value), the gas equilibration time is much less than 1 s. Pore filling with liquid butane will take longer than the gas equilibration time estimate due to the change in volume on condensation. The nanopore size distribution (2−10 nm) is such that these structures fill first at partial pressures < 0.1, and the total mass of butane in the pore is a small fraction of the total sorbed. Therefore, the majority of the mass uptake occurs on the outer surface.

Over most of the isotherm, typical pressure step changes took about 20 s to ramp up to 95% of the target value, followed by fine adjustments to reach the final pressure. The mass change of the sample closely tracked the pressure step change; there were only a few seconds (3−6) lag between the times needed to reach 95% of the new pressure value compared to that of the new mass value. The rapid uptake of butane during pressure steps was consistent with bulk flow to MWNT outer surfaces, followed by sorption. All the isotherms were of type II, which corresponds to adsorption on a nonporous solid. This is expected, since the inner surface area is significantly smaller than the outer (only 0.6−2.6% of the outer area). The sorption isotherms were reversible upon desorption: the weight uptake data matched to within 1% or less for the two curves. The adsorption/desorption isotherms show no indication of hysteresis for the samples. The pore sizes of these samples were strictly within the meso range (usually defined as the diameter range of 2−50 nm[23]). Solids with micropores (diameters < 2 nm) show hysteresis for butane.[24] Micropore-type behavior can be generated in powdered solids by compaction, which develops many particle-to-particle contacts that result in hysteresis while the same material previous to compression showed none.[25] Figure 2 shows that the MWNTs used in these experiments have few particle-to-particles contacts, eliminating this mechanism for hysteresis.

Several other researchers have noted the lack of hysteresis in the sorption of gases onto MWNTs: nitrogen[7,22] and methane.[22] However, hysteresis has been reported for nitrogen sorption on single-wall carbon nanotubes.[26,27] The morphologies of many single wall nanotube samples have many tube-to-tube contacts, including bundles. The lack of hysteresis on desorption provides an advantage to using MWNTs for recovery of condensable gases.

The physical adsorption of gases by nonporous solids gives rise to a type II isotherm (mesoporous range), which is often modeled using the BET equation. The isotherm for butane uptake on MWNT has been modeled in this manner after the pore condensation contribution was subtracted from the data. Pore condensation levels can be computed directly from the physical properties of butane (liquid density, vapor pressure, and surface tension; DIPPR[21]). Table 1 shows that pore condensation accounted for less than 1% of the uptake for all three samples. Furthermore, the pores were filled at very low butane partial pressures (about 5−10 mbar). The remainder of the butane sorption is assumed to be multilayer surface condensation. Alkane sorption on graphite surfaces has been previously investigated, and it is known that multilayer sorption occurs.[28−31] Butane is not likely to be adsorbing between the MWNT carbon layers. Butane's radius of gyration is 2.89 Å, while the distance between the carbon layers is 3.35 Å. For slit shaped pores, adsorption will occur when the diameter of the pore is greater than 1.5 $\sigma$, where $\sigma$ is the diameter of the adsorbate molecule.

**Sorption Model.** Two equations were used to model the uptake data: the BET equation (A) (Brunauer, Emmet, and Teller) and the modified BET equation (B), both given here below.

$$\frac{\frac{P}{P_0}}{n\left(1-\frac{P}{P_0}\right)} = \frac{1}{cn_m} + \frac{(c-1)\frac{P}{P_0}}{cn_m} \qquad \text{(A)}$$

$$\frac{k\frac{P}{P_0}}{n\left(1-k\frac{P}{P_0}\right)} = \frac{1}{cn_m} + \frac{k(c-1)\frac{P}{P_0}}{cn_m} \qquad \text{(B)}$$

The BET model correlates the relative pressure, $P/P_0$, and the surface uptake quantity, where $P$ is the system pressure, $P_0$ is the saturated vapor pressure, and $n$ (moles) is the surface uptake quantity. The BET model normally gives a good fit for a relative pressure in the range 0−0.3. Equation A assumes that an infinite layer thickness is possible, while the modified BET model uses $k$ to adjust for a limited number of layers. The constant, $n_m$, relates to the moles sorbed at monolayer coverage, which can be found at the point of inflection of the isotherm. The other two constants, $c$ and $k$, relate to the slope of the curve before and after multilayer adsorption takes place.

Table 2 shows the estimated number of butane multilayers for each sample at a relative pressure of 0.9. These numbers were calculated by using the MWNT morphology and the radius of gyration for butane. The smaller MWNTs have a higher number of layers, which is somewhat unexpected due to the negative radius of curvature of the MWNT surfaces. Butane multilayer volumes were also computed using the van der Waals surface area for butane and gave similar results.

The model coefficients and their average standard errors are given in Table 2 for the BET and the modified BET fits. As expected, the error of the BET model is larger over the total range, particularly for $P/P_0 > 0.3$ (Figure 8). The modified BET model gave the lower error when fitted to the experimental data. The modified BET equation is used specifically for multilayer sorption with the number of layers less than 10, as is the case with these data.

The butane sorbed at a monolayer coverage, $n_m$, can also be computed from first principles by knowing the surface area distribution of the samples and the radius

(23) Gregg, S. J.; Sing, K. S. W. *Adsorption, Surface Area and Porosity*, 2nd ed.; Academic Press: New York, 1982.
(24) Jagtoyen, M.; Derbyshire, F. *Carbon* **1993**, *31* (7), 1185.
(25) Avery, R. G.; Ramsey, J. D. F. *J. Colloid Interface Sci.* **1973**, *42*, 597.
(26) Yang, Q. H.; Fan, Y. Y.; Li, F.; Liu, C.; Liu, M.; Fan, Y. Z.; Cheng, H. M.; Wang, M. Z. Analysis of pore structure of carbon nanotube. Eurocarbon 1st world conference on carbon, 2000; Vol. II, pp 1025−1026.
(27) Eswaramoorthy, M.; Sen, R.; Rao, C. N. R. *Chem. Phys. Lett.* **1999**, *304*, 207.
(28) Piper, J.; Morrison, J. A. *Phys. Rev. B* **1994**, *30*, 3486.
(29) Hamilton, J. J.; Goodstein, D. L. *Phys. Rev. B* **1983**, *28*, 3838.
(30) Lysek, M. J.; LaMadrid, M. A.; Day, P. K.; Goodstein, D. L. *Phys. Rev. B* **1993**, *47*, 7389.
(31) Trabelsi, M.; Coulomb, J. P. *Surf. Sci.* **1992**, *272*, 352.

**Table 2. Experimental and Modeled Quantities of Butane Monolayer on MWNTs for VGB61, VGB62, and VGB63**

| sample | VGB61 | VGB62 | VGB63 |
|---|---|---|---|
| no. layers[a] ($P/P_0 = 0.9$) | 3.7 | 3.3 | 2.5 |
| monolayer[a] [g/m$^2$] | 3.59E−04[d] | 4.29E−04 | 4.85E−04 |
| $n_m$[b] [mol] | 1.01E−05 | 5.41E−06 | 3.29E−06 |
| $c$[b] | 99 | 127 | 184 |
| standard av error[b] ($P/P_0 = 0.9$) | 6.23E−12 | 1.84E−12 | 2.00E−13 |
| total standard av error[b] | 8.56E−08 | 8.73E−10 | 2.61E−09 |
| k[c] | 0.78 | 0.72 | 0.73 |
| $n_m$[c] [mol] | 1.00E−05 | 5.35E−06 | 3.25E−06 |
| c[c] | 162 | 125 | 136 |
| standard av error[c] | 3.18E−11 | 1.65E−12 | 2.30E−12 |

[a] Number of multilayers adsorbed onto MWNTs and amount of butane in the monolayer from experimental data. [b] BET equation constants and error for fit of the model to experimental data. Only data at $P/P_0 < 0.3$ were considered in determining the model coefficients. [c] Modified BET equation constants and error for fit of the model to experimental data. All data were considered in determining the modified BET model coefficients. [d] Read as $3.59 \times 10^{-4}$.

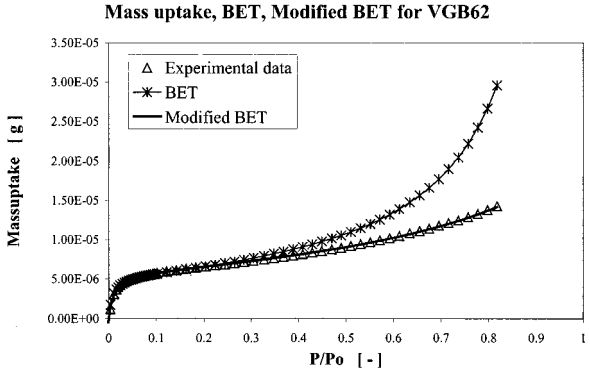


**Figure 8.** Comparison of BET and modified BET equations with VGB62 sorption data.

**Table 3. Comparison of $n_m$ (Monolayer Coverage) Estimated by Using Three Different Methods**

| sample | $n_m$ primary data calculations [g butane/g MWNT] | $n_m$ BET [g butane/ g MWNT] | $n_m$ modified BET [g butane/ g MWNT] |
|---|---|---|---|
| VGB61 | 1.37E−02[a] | 1.31E−02 | 1.30E−02 |
| VGB62 | 7.00E−03 | 1.12E−02 | 1.28E−02 |
| VGB63 | 5.43E−03 | 7.08E−03 | 6.96E−03 |

[a] Read as $1.37 \times 10^{-2}$.

of gyration (or van der Waals area) of butane. Table 3 shows the computed monolayer coverage and the BET and modified BET model coefficients. Clearly, these independently determined values agree very well. Butane monolayer coverage decreases on a g of butane/g of MWNT basis as the outside diameter increases. Recall that the butane sorption in the pores has been subtracted from the sorption data so that sorption on the inside tube walls is not considered.

Surface sorption of butane occurs despite the negative curvature of the MWNT surface. A simple multilayer quantity estimation, based on butane's radius of gyration and the assumption that the multilayer packing was as high as the monolayer packing, showed that the number of multilayers increased with decreasing MWNT diameter. The amount of sorbed butane on the MWNT external surfaces is affected by the attraction between the surface and the molecules, the local packing of the butane molecules in the condensed phase, and the vapor pressure of the butane at the liquid−gas interface. Butane vapor pressure at the liquid−gas interface should increase as the MWNT diameter decreases. In the absence of condensed phase packing differences or surface attraction differences, the surface curvature effect would lower the number of multilayers expected for nanotubes of smaller diameters at a given system pressure.

Differences in molecular packing in condensed films have been observed. Various studies on adsorption of rodlike molecules (such as butane or nitrogen) on flat graphite surfaces[32,33] show that the effective packing of the monolayer and the multilayers differ. The monolayer has a crystalline structure, while the multilayers are more loosely packed. Longer CH chains ($C > 3$) can switch between gauche and trans conformation while sorbed on graphite, thereby changing the effective packing as well. Also, butane molecules might be tilted relative to the graphite surface, sorbing primarily with only one end/carbon attached to the surface. These three mechanisms could result in different multilayer densities with different MWNT radii.

There is evidence that the interaction between a graphitic carbon surface and a sorbed molecule can increase as the surface becomes highly curved. The most highly twisted bonds on carbon fullerenes are preferred as reactive sites.[34] The $sp^2$ electrons of a flat graphitic surface are planar and fairly inert. Curving a "graphitic surface" would put strain on these orbitals; such strain could be reduced by interaction with molecules sorbed on the surface. Specifically, carbon nanotubes show enhanced reactivity in regions over which the tube surfaces are highly strained. Hydrogen[35] is computed to chemisorb preferentially onto folded surfaces of deformed nanotubes. Therefore, surfaces with more curvature could exhibit increased attraction energies for sorbed molecules, resulting in higher surface loadings and possibly different local packings.

## Conclusions

Butane sorbs on MWNTs by two mechanisms: pore condensation and surface condensation. Morphology data used in concert with the sorption data show that multilayer surface condensation accounted for most of the butane sorption. MWNTs with smaller outside diameters sorbed more butane, consistent with other findings that the strain in curved graphitic surfaces affects sorption and reaction. The butane was readily desorbed with no hysteresis because of the low volume fraction of mesopores in the samples. Rapid, reversible desorption would be of great advantage in processes involving adsorption of valuable or toxic compounds. Sorption isotherms were modeled using the modified BET equation, with monolayer coefficients consistent with those calculated directly from the sorbant properties and the MWNT morphology.

**Acknowledgment.** This work was supported by the Advanced Carbon Materials Center that is funded through the NSF-MRSEC program (DMR-9809686). S.B.S. acknowledges support from the NASA Ames Research Center.

LA010131T

(32) Herwig, K. W.; Wu, Z.; Dai, P.; Taub, H. *J. Chem. Phys.* **1997**, *107*, 5186.
(33) Herwig, K. W.; Newton, J. C.; Taub, H. *Phys. Rev. B* **1994**, *50*, 15287.
(34) Weedon, B. R.; Haddon, R. C.; Spielmann, H. P.; Meier, M. S. *J. Am. Chem. Soc.* **1999**, *121*, 335.
(35) Srivastava, D.; Brenner, D. W.; Schall, J. D.; Awman, K. D.; Yu, M.-F.; Ruoff, R. S. *J. Phys. Chem. B* **1999**, *103*, 4330.